

ChemComm

Accepted Manuscript



This article can be cited before page numbers have been issued, to do this please use: Y. Kitayama and M. Isomura, *Chem. Commun.*, 2018, DOI: 10.1039/C7CC09889H.



This is an Accepted Manuscript, which has been through the Royal Society of Chemistry peer review process and has been accepted for publication.

Accepted Manuscripts are published online shortly after acceptance, before technical editing, formatting and proof reading. Using this free service, authors can make their results available to the community, in citable form, before we publish the edited article. We will replace this Accepted Manuscript with the edited and formatted Advance Article as soon as it is available.

You can find more information about Accepted Manuscripts in the [author guidelines](#).

Please note that technical editing may introduce minor changes to the text and/or graphics, which may alter content. The journal's standard [Terms & Conditions](#) and the ethical guidelines, outlined in our [author and reviewer resource centre](#), still apply. In no event shall the Royal Society of Chemistry be held responsible for any errors or omissions in this Accepted Manuscript or any consequences arising from the use of any information it contains.



Journal Name

COMMUNICATION

Gas-Stimuli-Responsive Molecularly Imprinted Polymer Particles with Switchable Affinity for Target Protein

Received 00th January 20xx,
Accepted 00th January 20xx

DOI: 10.1039/x0xx00000x

Y. Kitayama^a M. Isomura^awww.rsc.org/

Gas-responsive molecularly imprinted polymer (MIP) particles, which have nanocavities in their shell layer for protein recognition, were developed for the first time. The MIP particles showed higher affinity for the target protein inside a CO₂-treated aqueous medium as compared to that under N₂-treated conditions, while retaining selectivity to the target protein.

Development of molecular recognition materials has been attracting much attention because of their significant contribution to various research and industrial fields, such as environmental analysis, protein purification, clinical diagnosis, sensors, drug monitoring, and therapy.¹⁻⁵ Genetically translated proteins such as antibodies and enzymes, which are known to show molecular recognition properties, are widely used in the above mentioned applications. However, these protein-based molecular recognition materials are fragile and unamenable for further functionalization. Artificial molecular recognition materials have great potential as alternatives to protein-based materials because of their high stability and facile production process.

Molecularly imprinted polymers (MIPs) are known to be promising artificial materials as substituents of natural antibodies.⁶⁻¹⁶ MIPs are synthesized by molecular imprinting; radical polymerization is carried out in the presence of template molecules that interact with functional molecules, co-monomers, and crosslinking agents to yield a polymer matrix around the template molecules. Subsequently, template removal from the crosslinked polymers furnishes MIPs bearing three-dimensional nanocavities that can recognize the target molecules whose sizes and shapes are complementary to those of the nanocavities. In a typical MIP synthesis, a wide range of vinyl monomers and initiators can be used as building blocks, and functional molecular recognition materials can be fabricated by using functional building blocks.^{7,11} Recently, a method for synthesizing stimuli-responsive MIPs was developed, wherein temperature, light, pH, biomolecule, ion and a

solvent was used as external stimuli for switching the recognition properties.¹⁷⁻²³ Furthermore, the stimuli responsive properties enabled MIPs to be used in various advanced applications, such as treatment of antibiotic-resistant bacteria, control of cell adhesives and programmable downregulation of enzyme activity.²⁴⁻²⁶

Herein, gas-stimuli responsive MIP particles having switchable recognition capability and respond to carbon dioxide (CO₂) and nitrogen (N₂) as gas stimuli have been developed (Scheme 1). We used a gas-responsive initiator, 2,2'-azobis[2-(2-imidazolin-2-yl)propane] (VA-061), which has imidazoline groups as a functional initiator (FI) that can target proteins for the preparation of gas-stimuli responsive MIP particles. In the molecular imprinting process, FI can interact to template molecules and decomposed to initiator radicals for starting the polymerization, and the initiator-derived functional groups must be introduced into the polymer chain end. After the polymerization of comonomer and crosslinking agent, the template removal resulted in the imprinted cavities bearing imidazoline groups as interaction sites derived from FI. Therefore, the initiator-derived functional groups may be used as interaction sites in the molecularly imprinted nanocavities. In this study, the imidazoline groups inside nanocavities are reacted with CO₂ dissolved in water, forming their bicarbonate salt. The reverse reaction proceeds by introducing N₂ gas.²⁷⁻³⁰ Therefore, the functional groups can be controlled from charged state to uncharged state via introducing CO₂ and N₂, respectively. If the molecular imprinting process was demonstrated in the CO₂-treated condition, the imprinted cavities were constructed with protonated imidazoline groups as interaction sites. Therefore, the affinity toward target molecules would be greater in CO₂-treated condition compared to N₂-treated condition in which unprotonated imidazoline groups are present in cavities as interaction sites. These gases are abundant, inexpensive, and non-toxic. In particular, the gas-responsive materials are advantageous over pH-responsive materials based on a conventional acid or base, because salt accumulation in the latter case weakens the response. More importantly, CO₂ is biocompatible because it is naturally generated in human cells as one of the important metabolites. Consequently, gas-responsive molecular recognition materials have great potential for use in bio-related applications. In this study, for the first time,

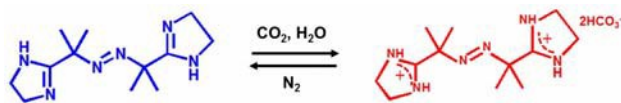
^a Graduate School of Engineering, Kobe University, 1-1, Rokkodai-cho, Nada-ku, Kobe 657-8501, Japan

Electronic Supplementary Information (ESI) available: [details of any supplementary information available should be included here]. See DOI: 10.1039/x0xx00000x

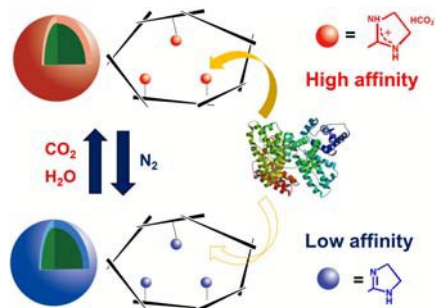
COMMUNICATION

Journal Name

gas stimuli were applied for the switchable molecular recognition properties of MIPs, where a protein with a fragile tertiary structure was used as the target molecule.



Scheme 1. Gas-responsive property of VA-061



Scheme 2. Gas-responsive core-shell MIP particles having a molecularly imprinted polymer shell layer.

Herein, human serum albumin (HSA) was selected as the model target protein. To investigate the gas responsiveness of VA-061, the chemical shifts were measured by $^1\text{H-NMR}$ using D_2O as the solvent after treating it with CO_2 and N_2 . The proton peaks derived from the ethylene moiety in the imidazoline groups ($\delta = 3.55$, before CO_2 treatment) were shifted toward lower magnetic fields after CO_2 bubbling ($\delta = 3.97$). However, subsequent N_2 treatment, the chemical shift was measured at higher magnetic fields ($\delta = 3.77$) (Figure S1). In the case of 2,2'-azobis[2-(2-imidazolin-2-yl)propane] hydrochloride (VA-044), the chemical shift of the proton peaks, which is due to the ethylene group in the imidazoline, remained unaffected after the CO_2 and N_2 introduction ($\delta = 3.85$ (Figure S2)). This indicated that deprotonation via gas introduction did not occur in the hydrochloride salt state but occurred in the bicarbonate salt state formed upon CO_2 introduction. These results revealed that the protonation and deprotonation states for VA-061 can be switched via CO_2 and N_2 gas treatment.

Gas-responsive core-shell type MIP particles were prepared using VA-061 as an FI by a two-step emulsifier-free emulsion polymerization; consequently, molecularly imprinted nanocavities were created only in the shell layer for high protein accessibility.³¹⁻³³ The seed particles were synthesized by the emulsifier-free emulsion polymerization of styrene (S) and divinylbenzene (DVB) with VA-061 in CO_2 -treated water. The z-average particle size (d_z) of P(S-DVB) particles was ~ 117 nm (zeta potential: +48 mV) (Figure S3). Subsequently, core-shell MIP particles, which contain molecular recognition nanocavities in the shell layer, were prepared by the emulsifier-free seeded polymerization of 2-hydroxyethyl methacrylate (HEMA) as a comonomer and N,N' -methylenebisacrylamide (MBAA) as a crosslinker using VA-061 as an FI. HSA (66 kDa, $\text{pI}=4.7$) was used as a template in the presence of P(S-DVB) seed particles dispersed in CO_2 -treated water at 40°C , where the template HSA was not denatured in CO_2 -treated water

(Figure S4). After the seeded polymerization was complete, the obtained particles were washed by centrifugation with an aqueous solution of a surfactant and tris(2-carboxyethyl)phosphine hydrochloride to remove the remaining monomer species and template HSA. The d_z value of the core-shell HSA-imprinted particles (HEMA-VA061_MIP) was ~ 158 nm (zeta potential: +25 mV), indicating that a molecularly imprinted polymeric shell layer of around 20 nm was successfully created. (Figure S5) Non-imprinted polymer (HEMA_VA061-NIP) particles, which served as reference particles, were also synthesized by the same procedure but in the absence of the template HSA.

To examine the binding activity, HSA was incubated with HEMA-VA061_MIP particles dispersed in the aqueous solution treated with CO_2 , and the amount of bound HSA was estimated by microBCA assay of the supernatant obtained after the centrifugal separation of the particles. The amount of HSA bound to the HEMA-VA061_MIP particles increased as the concentration of HSA increased. From the binding isotherm, the binding constant (K_a) was estimated to be $2.06 \times 10^7 \text{ M}^{-1}$ (Figure 1 and Figure S6). In addition, the affinity of the HEMA-VA061_MIP particles toward HSA was clearly higher than that of the HEMA-VA061_NIP particles ($K_a = 1.50 \times 10^6 \text{ M}^{-1}$) in the CO_2 -treated water. The bound amount of HSA increased linearly in the case of HEMA-VA061_NIP, which indicated that HSA was non-specifically bound to these particles. To estimate the effect of molecular imprinting, we adopted an imprinting factor (IF), which is defined as the ratio of the K_a values of MIP particles to that of NIP particles. The calculated value was approximately 13.7. Consequently, the molecular imprinting process was determined to be successful in the case of the HEMA-VA061_MIP particles.

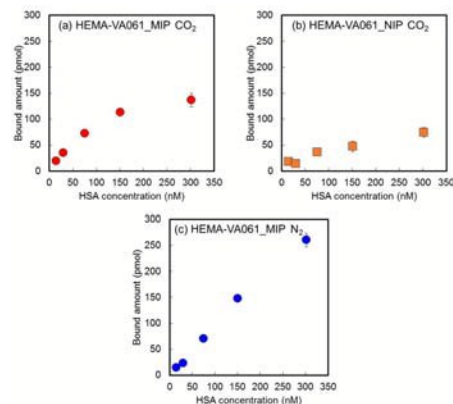


Figure 1. HSA binding isotherms of HEMA-VA061_MIP in CO_2 -treated aqueous phase (a), HEMA-VA061_NIP in CO_2 -treated aqueous phase (b), and HEMA-VA061_MIP in N_2 -treated aqueous phase (c). The particles were prepared at 40°C .

The selectivity of the HEMA-VA061_MIP particles to HSA was examined using reference proteins such as immunoglobulin G (IgG: 150 kDa, $\text{pI}=6.0 - 8.0$), cytochrome c (Cyt: 11 kDa, $\text{pI}=10.2$), and lysozyme (Lys: 14 kDa, $\text{pI}=11.1$). The evaluated selectivity factor (SF) values for the HEMA-VA061_MIP particles in CO_2 -treated water were 0.25, -0.11, and 0.04 in the case of IgG, Cyt, and Lys, respectively. (Figure 2) On the other hand, the HEMA-VA061_NIP particles did not show selective binding to HSA (0.67, 0.86, and 1.37 for IgG, Cyt, and Lys, respectively). These results indicated that the

HSA recognizing nanocavities were successfully formed in the HEMA-VA061_MIP particles via molecular imprinting.

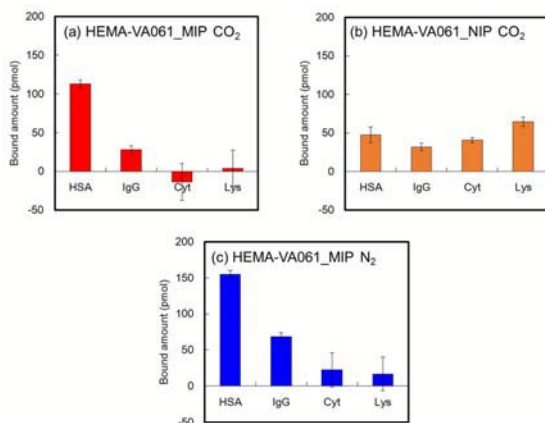


Figure 2. Results of the selectivity test of HEMA-VA061_MIP in CO₂-treated aqueous phase (a), HEMA-VA061_NIP in CO₂-treated aqueous phase (b), and HEMA-VA061_MIP in N₂-treated aqueous phase (c). The protein concentration was 150 nM. The particles were prepared at 40 °C.

To investigate the effect of polymerization temperature during the molecular imprinting process on the recognition properties of the HEMA-VA061_MIP particles, another batch of MIP particles was synthesized by the same procedure at 65 °C, and their binding affinity and selectivity were evaluated. It is known that the template HSA is not denatured below 70 °C.³⁴ The HEMA-VA061_MIP particles thus obtained had particle sizes and colloidal properties similar to those of the particles prepared at 40 °C. (Figure S7) From the HSA binding isotherm of the HEMA-VA061_MIP particles prepared at 65 °C, the binding affinity, K_a , was found to be $6.41 \times 10^6 \text{ M}^{-1}$ in the CO₂-treated water, which was 4.2 times greater than that of HEMA-VA061_NIP particles prepared at 65 °C (IF: 4.2, $K_a = 1.54 \times 10^6 \text{ M}^{-1}$). However the binding affinity was 3.2 times smaller than that of the MIP particles prepared at 40 °C ($K_a = 2.06 \times 10^7 \text{ M}^{-1}$). (Figures S8 and S9) The selective binding capability of the HEMA-VA061_MIP particles prepared at 65 °C was confirmed (0.06, 0.43, and 0.66 for IgG, Cyt, and Lys, respectively, in CO₂), but the selectivity was poorer when compared to that of the HEMA-VA061_MIP particles prepared at 40 °C. (Figure S10) These results indicate that the polymerization temperature is an important factor and that a lower polymerization temperature is favorable for creating nanocavities with precise recognition ability, high affinity, and high selectivity.

The gas-responsive properties of the HEMA-VA061_MIP particles were examined via binding experiments using CO₂- and N₂- treated aqueous solutions. First, to investigate the gas responsive colloidal properties of the HEMA-VA061_MIP particles, CO₂ treatment was carried out for 90 min, followed by N₂ treatment for 90 min. The d_z value of the MIP particles was similar during these gas treatments (~156 nm after CO₂ treatment and ~160 nm after N₂ treatment), whereas the zeta potential was clearly increased after CO₂ treatment (+37 mV) and the value was clearly decreased after the N₂ treatment (+17 mV). The zeta potential value after N₂ treatment was back to that before CO₂ treatment (+25 mV). (Figure S11) This indicated that the electrostatic properties of the shell layer of the

HEMA-VA061_MIP particles reversibly changed but the colloidal stability was maintained.

To evaluate the gas-responsive recognition properties of the HEMA-VA061_MIP particles prepared at 40 °C, a responsive factor (RF), defined as the ratio of the K_a values of the MIP particles in the CO₂-treated aqueous phase to that under N₂-treated conditions, was adopted. The affinity constant of these particles for HSA ($K_a = 8.78 \times 10^5 \text{ M}^{-1}$), which was estimated from the binding isotherm of the HEMA-VA061_MIP particles dispersed in N₂-treated water, was ~23 times smaller than that of the MIP particles in CO₂-treated water (RF: 23). (Figure 1) Thus, switching of the gas-based affinity was successfully demonstrated in the HEMA-VA061_MIP particles. The switching property should be caused by the gas-responsive property of interaction sites derived from FI between charged and uncharged states, and the reversibility could be repeated more than 3 times (Figure S12).

Furthermore, the SF values for HEMA-VA061_MIP particles prepared at 40 °C slightly worse in N₂-treated water, i.e., 0.44, 0.14, and 0.11 for IgG, Cyt, and Lys, respectively compared to CO₂-treated condition, but selective binding ability to HSA was maintained. (Figure 2) The results are reasonable because nanocavities showing affinity to HSA were formed via the molecular imprinting process, and the nanocavity structure was preserved during N₂ treatment. The interaction sites (imidazoline groups) were more active under the CO₂-treatment condition, which led to greater affinity and selectivity to HSA. It is worth noting that the gas-responsive molecular recognition property was also confirmed for HEMA-VA061_MIP particles prepared at 65 °C with similar gas-responsive colloidal property (Figure S13), i.e. the greater affinity toward HSA was confirmed in CO₂-treated water ($K_a = 6.41 \times 10^6 \text{ M}^{-1}$) than that for N₂-treated water ($K_a = 1.79 \times 10^6 \text{ M}^{-1}$), but the gas-responsiveness was clearly lower than that for HEMA-VA061_MIP-NPs prepared at 40 °C (Figure S9).

Since the polymer matrix constitutes nanocavities, the creation of nanocavities is independent of the comonomer species. However, the nature of the comonomers should influence the non-specific binding on the polymer matrix. To investigate the versatility of our proposed molecular imprinting process and the effect of the comonomer on the binding affinity, the selectivity and gas-responsive properties of the MIP particles, two additional water-soluble comonomers, i.e., *N*-isopropylacrylamide (NIPAm) and di(ethyleneglycol) methyl ether methacrylate (DEGMA), were used for the MIP particle synthesis. The MIP particles thus obtained had similar particle sizes (d_z values: 149 nm and 138 nm, respectively). (Figures S14) For all the MIP particles, saturable binding isotherms were observed under the CO₂-treatment conditions, whereas linear binding profiles were observed under the N₂-treatment conditions. (Figure 3) The estimated binding affinity values for the NIPAm-VA061_MIP and DEGMA-VA061_MIP particles in CO₂ were $K_a = 8.74 \times 10^6 \text{ M}^{-1}$ and $K_a = 1.03 \times 10^7 \text{ M}^{-1}$, respectively. The affinity values for both MIP particles decreased in N₂ ($K_a = 3.14 \times 10^6 \text{ M}^{-1}$ and $K_a = 1.40 \times 10^6 \text{ M}^{-1}$, respectively), where the RF values were 2.8 and 7.4, confirming gas responsiveness for all the comonomers used in this study. (Figures 3 and S15) The SF values in the case of the MIP particles using NIPAm in CO₂ were 0.34, 0.74, and 0.85 for IgG, Cyt,

and Lys, respectively. The corresponding values for the MIP particles using DEGMA were 0.38, 0.39, and 0.71 in the case of IgG, Cyt, and Lys. (Figure 3) These results indicated that all MIP particles prepared using the three different comonomers showed HSA-specific binding capability with gas-responsive recognition property, and that molecular imprinting with FI could be applied to the various comonomers. The smallest extent of non-specific binding of off-target proteins was confirmed in the HEMA-VA061_MIP particles, which may be due to the highest hydrophilicity of this comonomer among the selected comonomers in this study, i.e., the logP values estimated by Pallas were 0.54 for HEMA, 0.87 for NIPAm, and 1.01 for DEGMA. The worse K_a and SF values for NIPAm-VA061_MIP particles may be caused by the non-specific binding based on the hydrogen bonding to amide group in NIPAm. Therefore, selection of the appropriate hydrophilic comonomer is important for precise molecular recognition due to the decrease in the non-specific binding of the off-target proteins.

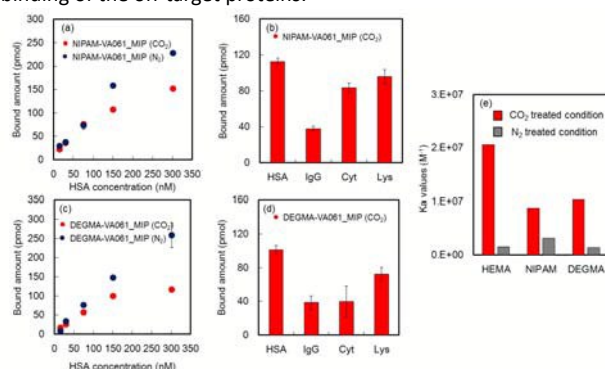


Figure 3 HSA binding isotherms in CO₂- and N₂-treated water (a, c) and selectivity test of NIPAm-VA061_MIP (b) and DEGMA-VA061_MIP (d). The particles were prepared at 40 °C. Affinity constants estimated from binding isotherm of HSA for HEMA-VA061_MIP, NIPAm-VA061_MIP, and DEGMA-VA061_MIP to HSA in CO₂- and N₂-treated water (e).

In conclusions, novel gas-stimuli responsive core-shell MIP particles having nanocavities in the shell layer that are capable of molecular recognition were successfully synthesized. A gas-responsive initiator was used as a functional molecule that interacted with a specific target protein. The affinity toward this target protein was controlled by the introduction of gases having selective binding properties. Greater affinity was observed in the CO₂-treated aqueous phase as compared to that under N₂-treatment conditions. Furthermore, the versatility of the molecular imprinting process, which used a gas-responsive FI for gas-responsive MIP synthesis, was successfully confirmed by using different types of comonomers. We believe that the gases act as better stimulants than other stimuli because gases like CO₂ and N₂ are abundant, inexpensive, and non-toxic. In addition, CO₂ is a key metabolite in cells and helps in maintaining the intracellular pH. Therefore, we hope that the aforementioned gas-based stimuli-responsive molecular recognition materials will be used in various biological applications, such as reversible affinity chromatography, reusable sensors, functional substrates for cell adhesive control, and analytical tools for cells to identify metabolic disorders.

The authors deeply appreciate Prof. Toshifumi Takeuchi for his fruitful discussion. This work was supported by JSPS KAKENHI (Grant number 25870429) and partially supported by Hosokawa Powder Technology Foundation, Japan and Kawanishi Memorial Shin Meiwa Education Foundation, Japan.

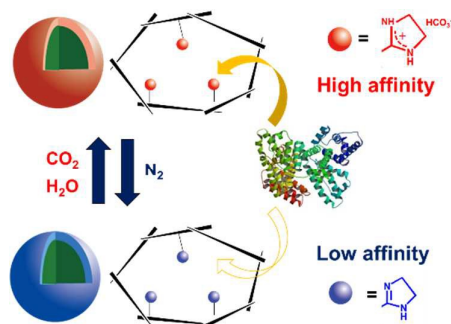
Conflicts of interest

There are no conflicts to declare.

Notes and references

1. C. Souriau and P. J. Hudson, *Expert Opin. Biol. Ther.*, 2001, **1**, 845.
2. A. Sassolas, B. D. Leca-Bouvier and L. J. Blum, *Chem. Rev.*, 2008, **108**, 109.
3. K. Tawa, F. Kondo, C. Sasakawa, K. Nagae, Y. Nakamura, A. Nozaki and T. Kaya, *Anal. Chem.*, 2015, **87**, 3871.
4. Y. Jiang, M. L. Shi, Y. Liu, S. Wan, C. Cui, L. Q. Zhang and W. H. Tan, *Angew. Chem. Int. Ed.*, 2017, **56**, 11916.
5. T. A. Waldmann, *Science*, 1991, **252**, 1657.
6. K. Haupt, *Molecular imprinting*, Springer, Berlin, 2012.
7. T. Takeuchi, H. Sunayama, E. Takano and Y. Kitayama, in *Molecularly imprinted polymers in biotechnology*, eds. B. Mattiasson and L. Ye, 2015, vol. 150, pp. 95-106.
8. D. E. Hansen, *Biomaterials*, 2007, **28**, 4178.
9. K. Mosbach, *Trends Biochem. Sci.*, 1994, **19**, 9.
10. G. Wulff, *Angew. Chem. Int. Ed. Engl.*, 1995, **34**, 1812.
11. R. Horikawa, H. Sunayama, Y. Kitayama, E. Takano and T. Takeuchi, *Angew. Chem. Int. Ed.*, 2016, **55**, 13023.
12. A. Kawamura, T. Kiguchi, T. Nishihata, T. Urugami and T. Miyata, *Chem. Commun.*, 2014, **50**, 11101.
13. K. Takimoto, E. Takano, Y. Kitayama and T. Takeuchi, *Langmuir*, 2015, **31**, 4981.
14. T. Takeuchi, T. Mori, A. Kuwahara, T. Ohta, A. Oshita, H. Sunayama, Y. Kitayama and T. Ooya, *Angew. Chem. Int. Ed.*, 2014, **53**, 12765.
15. Z. J. Zhang, Y. J. Guan, M. Li, A. D. Zhao, J. S. Ren and X. G. Qu, *Chem. Sci.*, 2015, **6**, 2822.
16. Z. J. Zhang, M. Li, J. S. Ren and X. G. Qu, *Small*, 2015, **11**, 1258.
17. Y. Kanekiyo, R. Naganawa and H. Tao, *Angew. Chem. Int. Ed.*, 2003, **42**, 3014.
18. Z. Y. Chen, L. Xu, Y. Liang and M. P. Zhao, *Adv. Mat.*, 2010, **22**, 1488.
19. W. T. Wu, J. Shen, Y. X. Li, H. B. Zhu, P. Banerjee and S. Q. Zhou, *Biomaterials*, 2012, **33**, 7115.
20. W. Chen, Y. Ma, J. M. Pan, Z. H. Meng, G. Q. Pan and B. Sellergren, *Polymers*, 2015, **7**, 1689.
21. K. Yoshimatsu, B. K. Lesel, Y. Yonamine, J. M. Beierle, Y. Hoshino and K. J. Shea, *Angew. Chem. Int. Ed.*, 2012, **51**, 2405.
22. W. Bai, N. A. Gariano and D. A. Spivak, *J. Am. Chem. Soc.*, 2013, **135**, 6977.
23. M. Watanabe, T. Akahoshi, Y. Tabata and D. Nakayama, *J. Am. Chem. Soc.*, 1998, **120**, 5577.
24. G. Q. Pan, Q. P. Guo, Y. Ma, H. L. Yang and B. Li, *Angew. Chem. Int. Ed.*, 2013, **52**, 6907.
25. W. Li, K. Dong, J. S. Ren and X. G. Qu, *Angew. Chem. Int. Ed.*, 2016, **55**, 8049.
26. Z. J. Zhang, Z. Z. Wang, F. M. Wang, J. S. Ren and X. G. Qu, *Small*, 2015, **11**, 6172.
27. D. H. Han, X. Tong, O. Boissiere and Y. Zhao, *ACS Macro Lett.*, 2012, **1**, 57.
28. X. Su, P. G. Jessop and M. F. Cunningham, *Macromolecules*, 2012, **45**, 666.
29. C. I. Fowler, P. G. Jessop and M. F. Cunningham, *Macromolecules*, 2012, **45**, 2955.
30. Y. X. Liu, P. G. Jessop, M. Cunningham, C. A. Eckert and C. L. Liotta, *Science*, 2006, **313**, 958.
31. A. Uchida, Y. Kitayama, E. Takano, T. Ooya and T. Takeuchi, *RSC Adv.*, 2013, **3**, 25306.
32. N. Murase, S. Taniguchi, E. Takano, Y. Kitayama and T. Takeuchi, *J. Mat. Chem. B*, 2016, **4**, 1770.
33. N. Murase, S. I. Taniguchi, E. Takano, Y. Kitayama and T. Takeuchi, *Macromol. Chem. Phys.*, 2015, **216**, 1396.
34. T. Takeuchi, Y. Kitayama, R. Sasao, T. Yamada, K. Toh, Y. Matsumoto and K. Kataoka, *Angew. Chem. Int. Ed.*, 2017, **56**, 7088.

Table of Contents



Molecularly imprinted polymer particles bearing gas-responsive property was successfully prepared using functional initiator